Asymmetry, cytoarchitectonic morphology, and genetics associated with Broca's area in schizophrenia

Saskia Zimmermann, MSc¹, Katrin Sakreida, PhD¹, Sebastian Bludau, PhD², Julia A. Camilleri, PhD^{3,4}, Felix Hoffstaedter, PhD³, Dominique I. Pelzer, B.Sc.², André Aleman, PhD⁵, Torsten Brückner, MD^{6,7}, Birgit Derntl, PhD⁸, Elmar Frank, MD⁶, Thomas Frodl, MD^{1,6,9}, Paola Fuentes-Claramonte, PhD^{10,11}, María Ángeles García-León, PhD^{10,11}, Oliver Gruber, MD¹², Göran Hajak, MD^{6,13}, Stefan Heim, PhD^{1,2}, Renaud Jardri, MD, PhD¹⁴, Lydia Kogler, PhD⁸, Peter M. Kreuzer, MD⁶, Daniela Mirlach, MD⁶, Michael Landgrebe, MD^{6,15}, Berthold Langguth, MD⁶, Edith Pomarol-Clotet, PhD^{10,11}, Julia Prasser, MD⁶, Martin Schecklmann, PhD⁶, Kang Sim, MBBS, MMed¹⁶, Joan Soler-Vidal, MD^{10,11,17,18}, Iris E. Sommer, MD, PhD¹⁹, Juan H. Zhou, PhD²⁰, Thomas W. Mühleisen, PhD^{2,21}, Simon B. Eickhoff, MD^{3,4}, Timm B. Poeppl, MD, MHBA^{1,6*}

- ¹ Department of Psychiatry, Psychotherapy and Psychosomatics, Medical Faculty, RWTH Aachen University, 52074 Aachen, Germany
- Institute of Neuroscience and Medicine, Structural and Functional Organization of the Brain (INM-1), Research Centre Jülich, 52428 Jülich, Germany
- ³ Institute of Neuroscience and Medicine, Brain and Behaviour (INM-7), Research Centre Jülich, 52428 Jülich, Germany
- Institute of Systems Neuroscience, Medical Faculty, Heinrich-Heine-University Düsseldorf, 40225 Düsseldorf, Germany
- Department of Neuroscience, University of Groningen, University Medical Center Groningen, 9700 AB Groningen, The Netherlands
- ⁶ Department of Psychiatry and Psychotherapy, University of Regensburg, 93053 Regensburg, Germany
- ⁷ District Hospital Rehau, 95111 Rehau, Gemany
- Department of Psychiatry and Psychotherapy, Tübingen Centre for Mental Health (TüCMH), Medical Faculty, University of Tübingen, 72016 Tübingen, Germany
- Department of Psychiatry and Psychotherapy, Otto von Guericke University Magdeburg, 39120 Magdeburg, Germany
- ¹⁰ FIDMAG Hermanas Hospitalarias Research Foundation, 8830 Sant Boi de Llobregat, Spain
- ¹¹CIBERSAM (G15), 08035, Barcelona, Spain
- ¹²Section for Experimental Psychopathology and Neuroimaging, Department of General Psychiatry, Heidelberg University, 69115 Heidelberg, Germany
- ¹³ Department of Psychiatry, Psychosomatic Medicine and Psychotherapy, Social Foundation Bamberg, 96049 Bamberg, Germany
- ¹⁴Université de Lille, INSERM U-1172, Lille Neurosciences & Cognition, Plasticity & Subjectivity Team, 59045
 Lille, France
- ¹⁵Department of Psychiatry, Psychotherapy and Psychosomatics, kbo-Lech-Mangfall-Klinik Agatharied Hausham, 83734 Hausham, Germany
- ¹⁶West Region, Institute of Mental Health, 539747 Singapore, Singapore
- ¹⁷Universitat de Barcelona, 08007 Barcelona, Spain
- ¹⁸Benito Menni Complex Asistencial en Salut Mental, 08830 Sant Boi de Llobregat, Spain
- ¹⁹ Department of Biomedical Science of Cells and Systems, University of Groningen, University Medical Center Groningen, 9713 GZ Groningen, The Netherlands
- ²⁰Centre for Sleep and Cognition & Centre for Translational Magnetic Resonance Research, Yong Loo Lin School of Medicine, National University of Singapore, 117549 Singapore, Singapore
- ²¹Cécile and Oskar Vogt Institute for Brain Research, Medical Faculty, University Hospital Düsseldorf, Heinrich Heine University Düsseldorf, 40225 Düsseldorf, Germany

*Corresponding Author: Timm B. Poeppl, MD, MHBA, Department of Psychiatry and Psychotherapy, Faculty of Medicine, University of Regensburg, Universitätsstraße 84, 93053 Regensburg, Germany (timm.poeppl@klinik.uni-regensburg.de).

Abstract

A common hypothesis on the etiopathology of schizophrenia is that the failure of segregation of right from left hemisphere functions is a core deficit in psychosis. It has even been proposed that schizophrenia symptoms in general may reflect a hemispheric 'dominance failure' for language and that the corresponding predisposition is genetic. Here, we show that reduced asymmetries of cytoarchitectonic Broca's subareas link to the degree of specific psychopathology and that specific gray matter reductions of subareas are related to a cognitive and a negative subtype of schizophrenia. Gene expression analyses indicate an upregulation of the *MET* gene in these particular areas, which has been implicated in neurodevelopment as well as neurocognition and influences the risk for schizophrenia. Our integrative findings suggest that variations of *MET* are associated with distinct structural alterations at the subregional level in key language regions, which may contribute to development of specific psychopathology in schizophrenia.

Introduction

With a heritability of 79% [1], schizophrenia has a strong genetic component. A variety of etiological factors such as genetic variations but also psychological experiences contribute to path-ophysiological neural processes that are mirrored in structural and functional brain alterations. These, in turn, likely promote impairments in fundamental cognitive processes. In particular, language impairments are a characteristic feature of schizophrenia [2,3] and are hence assessed as "disorganized speech" in established symptom scales. A common hypothesis on the etiopathology of schizophrenia is that the core deficit in psychosis is a failure of segregation of right from left hemisphere functions [4]. It has even been proposed that schizophrenic symptoms in general may reflect a hemispheric 'dominance failure' for language [5].

It has been assumed that communication impairments in schizophrenia are linked to abnormalities in higher cognitive functions such as working memory and executive control as well as impaired semantic and phonological processes [6-8]. Findings from neuroimaging studies in schizophrenia substantiate this assumption by demonstrating structural alterations in semantic and phonological brain networks [9-11]. Such abnormalities in language-related brain regions are even present in individuals with ultra-high risk for psychosis [12,13]. In first episode psychosis, volume reductions appear left lateralized and tend to spread bilaterally with progression of disease [12]. In this context, especially Broca's region is a suspect of disturbing related neural networks, due to its involvement in both language-specific and domain-general networks and its crucial role in both higher cognitive and language processing [14]. It is hence of particular interest to investigate whether and to what extent specific alterations in Broca's structural integrity are related to schizophrenic symptoms. Reports of previous imaging research into the relationship between alterations of gray matter volume in Broca's region and distinct schizophrenic symptoms such as disorganization, formal thought disorder, positive and negative symptoms are heterogeneous [15-17]. Most studies pointed to bilateral volume loss associated with varied schizophrenic symptoms [9,15,18], whereas results from one study indicated increased volume of Broca's region in formal thought disorder [19].

Beyond mere volumetric changes, anomalies in cerebral asymmetry were reported in individuals with schizophrenia. These were interpreted as a developmental failure, presumably influenced by genetic predisposition [5,20]. Since language abilities and hence arguably also key areas of language processing underlie strong hemispheric dominance, it seems worthwhile to investigate structural asymmetry of Broca's region in patients with schizophrenia. Previous studies provide equivocal and inconsistent evidence for either increased leftward asymmetry [21] but also of reversed, i.e., more rightward asymmetry in the pars triangularis (roughly corresponding to area 45) [22].

This heterogeneity of findings may be due to relatively small sample sizes and also due to methodological inconsistencies such as variability in anatomical definition of Broca's region and its subparts. Moreover, intersubject variability in sulcal contours defining anatomical boundaries is a challenging problem in generating a standard definition of Broca's region (and its homolog) [23]. Particularly in patients with schizophrenia, there is a high degree of interindividual variability of regional brain volumetric measurements [24]. Cytoarchitectonic 3D probability maps overcome these issues by providing regional parcellation on a microstructural level based on cytoarchitectonic boundaries. Moreover, they account for interindividual differences in a stereotactic space [25]. Unfortunately, an investigation of volumetric changes and asymmetry in Broca's region of schizophrenia patients using observer-independent cytoarchitectonic mapping is still missing.

It has been presumed that the delineated neuroanatomical abnormalities associated with schizophrenic symptoms are "a manifestation of genetic diversity in the evolution of the specifically human characteristic of language" [5]. Genome-wide association studies (GWAS) have identified 145 schizophrenia-related loci, each with a small contribution to risk, whose products are involved in neuronal development, transmission, and plasticity [26,27]. Among these genes, there is a group that has been implicated with language development and impairment. These genes in turn are thus candidates for language dysfunction and related psychopathological symptoms in schizophrenia that are mediated by neural aberrances [28]. There is, however, no study that investigated deviations of the expressions of language-related candidate genes in key areas of the language network (such as Broca's region) that might contribute to symptoms characteristic of schizophrenia. Yet, knowledge on such gene—brain structure—symptom relationships is essential for further development not only of etiopathology-related specific therapeutic strategies but also of measures that potentially prevent particular high-risk cohorts from transition to schizophrenia.

In sum, the available literature strongly points to a genetic mediation of structural alterations including asymmetry in Broca's region that substantially contribute to typical symptoms of schizophrenia. However, findings on volumetric changes and their relationship to psychopathology are heterogeneous, most likely due to small sample sizes and inconsistent anatomical delineation. In addition, the genetic basis of putative brain abnormalities and hence associated behavioral abnormalities is unknown. In other words, the exact relationship between genetic mechanisms, structural alterations in Broca's region and specific schizophrenic symptoms remains unclear. Here, we aimed to characterize the role of Broca's region in schizophrenia in more detail. For this purpose, we used cytoarchitectonically informed probability maps reflecting the interindividual variability to investigate subregional alterations of volume and asymmetry in Broca's region among a large sample of schizophrenia patients. We then assessed their relationship with psychotic symptoms on basis of a recently identified, data-driven factor structure of schizophrenia psychopathology. To identify candidate genes that may mediate these structure-symptom relationships, we combined cytoarchitectonic maps with RNA expression data for evaluating the regional specificity of gene activity.

Results

Gray matter volume and its association with symptoms

We first used region-based morphometry to test for gray matter differences between patients and comparison subjects within individual left and right cytoarchitectonic areas 44 and 45 (i.e., four regions). ANCOVA revealed only a main effect of group ($F_{1,474} = 31.403$; p < 0.001, $\eta_p^2 = 0.062$). There was a significant interaction group × hemisphere ($F_{1,474} = 7.922$; p = 0.005, $\eta_p^2 = 0.016$). Also, the group × cytoarchitectonic area × hemisphere ($F_{1,474} = 19.011$; p < 0.001, $\eta_p^2 = 0.039$) interaction yielded statistical significance. We then conducted post hoc t-tests to compare group means (Table 1). These revealed significantly reduced gray matter volume of all four areas in patients (Fig. 1B). The strongest effect of group was found for left area 45 ($t_{476} = 5.908$; p < 0.001, d = 0.540). For right area 45 ($t_{476} = 5.075$; p < 0.001, d = 0.464) and left area 44 ($t_{476} = 5.352$; p < 0.001, d = 0.491), small to medium effect sizes were observed. Right area 44 showed the smallest effect ($t_{476} = 3.245$; p = 0.001, d = 0.297). These results could be reproduced in a replication sample (see Supplementary Results).

To investigate whether the observed cytoarchitectonic-specific reductions relate to psychopathology, we correlated volumetric estimates with symptom severity in patients (Table 2). These analyses revealed a significant negative correlation between the domain of negative symptoms and volume of left areas 44 (r_s = -0.177, p = 0.003; Fig. 2A) and 45 (r_s = -0.157, p = 0.008; Fig. 2B). Severity of cognitive symptoms was associated with reduced volume of right area 45 (r_s = -0.150, p = 0.011; Fig. 2C). These results also remained significant when controlling for medication and disease duration (left area 44: r_s = -0.194, p = 0.003; left area 45: r_s = -0.164, p = 0.011; right area 45: r_s = -0.150, p = 0.018). There were no significant correlations between the cytoarchitectonic subregions of Broca's area and positive or affective symptoms. The associations between the domain of negative symptoms and left area 44 as well as between severity of cognitive symptoms and right area 45 also remained significant in our replication sample (left area 44: r_s = -0.147, p = 0.045; left area 45: r_s = -0.098, p = 0.130; right area 45: r_s = -0.166, p = 0.028).

Functional characterization

To obtain an objective description of the tasks recruiting areas that feature significantly reduced gray matter associated with symptom dimensions and thus provide a link to the psychopathology of schiz-ophrenia, we conducted a functional characterization of the areas that were significant in our correlation analysis (see Table 2). Hereby, psychological terms were related to the respective area as registered in the BrainMap database, that is, on basis of functional experiments in healthy individuals. Left areas 44 and 45 were significantly associated with various domains of language cognition

but also paradigms of reward and emotion processing (Supplementary Fig. 1, 2). In contrast, right area 45 was significantly associated with the domain cognition (including attention and social cognition) and corresponding semantic/face monitoring/discrimination tasks (Supplementary Fig. 3). Taken together, these associations derived from healthy participants corroborate the reported morphology–symptom relationships in our schizophrenia sample.

Asymmetry of gray matter

Al values were positive for area 44 across the whole sample (i.e., patients and controls), demonstrating a leftward asymmetry. In contrast, Al values in all participants were negative for area 45, indicating a general rightward asymmetry. Group comparisons showed that the magnitude of area 45 rightward asymmetry was significantly reduced in the patient sample with a small effect (t_{476} = 2.062; p = 0.04, d = 0.198). In contrast, there were no significant group differences in asymmetry of area 44 (t_{476} = 0.687; p = 0.492, d = 0.056). In the replication sample, there were no significant group differences in asymmetry of area 45 (t_{247} = 0.592; p = 0.554, d = 0.075), while magnitude of area 44 leftward asymmetry was significantly reduced in the patient sample with a small effect (t_{247} = 2.062; p = 0.026, d = 0.287). Of note, mean absolute Al values were generally smaller in patients for all comparisons, indicating reduced asymmetry. To test whether these specific effects can be explained by psychopathology, we assessed the relationship between Al values and the severity of the four psychotic symptom dimensions. Asymmetry of area 45 was positively correlated with the positive symptoms dimension (r_s = 0.160, p = 0.014), asymmetry of area 44 was negatively correlated with the cognitive (r_s = -0.273, p = 0.001) symptoms dimension. That is, the more severe the symptoms on the corresponding dimension, the more reduced the asymmetry in patients was.

Gene expression

The all-probes analyses revealed significant expression differences of two genes: MET and SIRT1 (Fig. 3). Comparisons between Broca's subparts and the left premotor area revealed significantly higher expression levels for MET in left areas 44 (p_{FWE} = 0.005; Supplementary Table 5) and 45 (p_{FWE} < 0.001; Supplementary Table 6). In the right hemisphere, MET was significantly more highly expressed in area 45 (p_{FWE} = 0.004; Supplementary Table 8). In contrast, SIRT1 was upregulated only in left area 45 (p_{FWE} = 0.037; Supplementary Table 6). None of the candidate genes was upregulated in right area 44 (Supplementary Table 7). Apart from one marginally significant effect in left area 44, the control analysis demonstrated no differential expression of color genes in areas 44 and 45 versus premotor areas on both hemispheres, supporting the relative specificity of regional expressions of MET and SIRT1 (Supplementary Tables 9–12).

Discussion

Here, we combined probabilistic cytoarchitectonic mapping, region-based morphometry, data-driven clustering of symptoms and gene expression analysis targeting Broca's region (and its homolog) to assess gene-brain structure-symptom relationships in schizophrenia.

On the basis of cytoarchitectonic atlases, region-based morphometry revealed a gray matter decrease in all four subregions, i.e., areas 44 and 45 on both hemispheres, in patients diagnosed with schizophrenia. This finding indicates that not only Broca's area but also its right-hemispheric homolog is affected in schizophrenia and might thus contribute to corresponding psychopathology. That we observed effects in all four cytoarchitectonic areas matches well with previous evidence from a small-sized manual tracing study that identified significant gray matter volume reduction of both Brodmann area 44 and 45 in patients with schizophrenia [18]. There is meta-analytic evidence that left area 44 and bilateral area 45 are integral parts of the healthy functional language network and are typically impaired in aphasia [29]. More specifically, they represent nodes of a left-lateralized multimodal semantic control network, which also comprises right area 45 as a right-hemispheric hub [30]. It might thus be conjectured that the observed gray matter reductions in key hubs of the language network lead to cognitive-communication deficits in schizophrenia, possibly with a specific effect on semantic cognition.

This inference seems particularly reasonable, given that the degree of gray matter reduction in right area 45 significantly correlates with the dimension of cognitive symptoms in patients. Although a priori not necessarily specific to Broca's area, this relationship was corroborated by our functional decoding analysis in healthy subjects which linked this area to attentional and social cognition as well as semantic and face discrimination tasks, which may point to the impact of alterations in right area 45 on socio-cognitive impairments in schizophrenia. According to more detailed findings from data-driven, coactivation-based parcellation in combination with functional decoding, right area 45 is functionally organized in two clusters: i) a dorsal cluster that is associated with cognitive reasoning and connected to a neural network for higher order executive task processing, planning and monitoring of goal-oriented behavior and higher cognitive operations; and ii) a ventral cluster that is linked with social cognition as well as with emotion processing and features a functional connectivity profile that similarly involves regions for higher-level social-cognitive functions and emotional processing [31]. Notably, a recent machine-learning study showed that intrinsic connectivity patterns of particularly a socio-affective network and the theory-of-mind network (which includes right area 45) [32] allow individual prediction of cognitive symptom dimension in schizophrenia [33]. Interestingly, the most predictive network nodes tracked with higher dopamine synthesis capacity [33]. These relationships are especially intriguing because impairment of theory of mind, as a crucial socio-cognitive aspect of communication and interaction, seems genuinely connected to difficulties in processing the pragmatic aspects of language (and not to impairment of general cognitive abilities such

as intelligence or executive functions) in patients with schizophrenia [6,16,34]. The observed correlative relationship between cytoarchitectonically informed morphology of right area 45 and the cognitive dimension of schizophrenic symptoms thus extends previous findings by suggesting that structural alterations may underlie the recently reported relationship between altered neural networks and psychopathology in the cognitive domain [33].

We did not observe a relationship between the positive symptoms dimension and gray matter alterations of Broca's subregions in patients with schizophrenia, despite previous evidence of the involvement of Broca's area in auditory-verbal hallucinations [35,36]. However, previous meta-analyses of *structural* brain alterations did not link auditory-verbal hallucinations to Broca's area but to left insula and superior temporal gyrus [37,38,39]. In contrast, meta-analyses of brain *function* indicated increased brain activity in neural networks including Broca's area [40,41]. Here, we report a relationship between reduced asymmetry of area 45 and severity of positive symptoms. Taken together, it might therefore be inferred that reduced asymmetry of a cytoarchitectonic subregion within Broca's area entailing functional disturbances rather than mere structural abnormalities of Broca's area originate and predict auditory-verbal hallucinations in schizophrenia [42,43].

On the left hemisphere, our morphometric analyses identified a significant correlation of both area 44 and 45 with negative symptoms. Prima facie, this finding might seem surprising, given neuroimaging evidence for an association between activation of this area and language-related processes such as phonology, semantics, overt and covert speech [44]. Our functional decoding analysis confirmed the link to domains of language cognition but also revealed associations with reward and emotion processing. In addition, lesion mapping investigations indicate its importance for linguistic processes linked to emotion: that is, damage to these regions impairs recognition of emotions conveyed by facial expressions by interfering primarily with lexical processing [45]. In this context, it is also noteworthy that left area 44 is an integral part of the mirror neuron system [46,47], which subserves theory of mind [48,49], which is typically impaired in schizophrenia [50,51], Deficits in this regard may be the result of structural alterations [52] and consequently functional dysconnectivity of left area 44 [53], which was also linked to theory of mind tasks in our functional characterization analysis. There is not only evidence that dysfunction in the mirror neuron system is associated with a decrease in emotional expression and reactivity in schizophrenia [54], but also that it influences severity of negative symptoms [50]. The observed correlation of gray matter loss with negative symptoms observed in our study is thus plausible, and it can be hypothesized that it results in the typical negative symptoms such as poverty of speech, emotional withdrawal, and blunted affect.

The here reported left-hemispheric correlation of area 44 and area 45 morphology with the negative symptom dimension apparently also conflicts with the popular theory that the right hemisphere is dominant in emotional expression (while the left hemisphere is dominant in language). However, it fits well with the more detailed notion that the right hemisphere processes primary emotions (e.g., fear) while the left hemisphere is important for preprocessing social emotions [55]. Our

analysis of the relationship between asymmetry and psychopathology suggests that reductions not only in volume but also in asymmetry impact specific symptoms. Hence, the seeming discrepancy regarding lateralization could also be resolved when considering the reduced asymmetry, which we found in patients with schizophrenia. In other words, the observed association between (impairment of) emotion/reward and (altered prefrontal morphology in) the left hemisphere as well as (impairment of) cognition and (altered prefrontal morphology in) the right hemisphere could just mirror a failure of hemispheric dominance. This assertion coincides with considering individuals who fail to develop cerebral lateralization to have a high risk for psychosis [5,20].

In fact, our gene expression analysis identified upregulation of a gene in all areas correlated with schizophrenic symptom dimensions that is related to cerebral lateralization processes: The MET gene belongs to the tyrosine kinase receptor family, which regulates a multitude of biological processes including growth, differentiation, adhesion, motility, and death [56]. MET is critical during neurodevelopment to ensure that neurons grow and migrate to position themselves in the appropriate location in the human cortex. Its transcription, in turn, is regulated by FOXP2, a gene that is implicated in regulating higher cognitive functions including language [57]. It has, for instance, been shown that FOXP2 variation modulates functional hemispheric asymmetries for speech perception [58]. Supplementary analyses (Supplementary Tables 13–16) suggested an upregulation of FOXP2 in Broca's subarea 44, which may support the previous notion that FOXP2 polymorphisms are associated with auditory-verbal hallucinations in schizophrenia [59,60]. Variations within the MET gene are suggested to lead to a decreased pathway activity during critical periods of neurodevelopment. In line with this notion, a genotyping study demonstrated that MET variation influences schizophrenia risk and neurocognition, which points to a neurodevelopmental role across phenotypes relevant to the central nervous system [61]. Another recent study found hyperconnectivity between Broca's region and right-hemispheric regions in drug-naïve early-stage schizophrenia, which were strongly associated with polygenic risk scores obtained from FOXP2-related genes including MET [62]. The finding of dysconnectivity was interpreted as related to disrupted lateralization of schizophrenia patients, which in turn may be associated with the language gene cluster, previously shown to account for language lateralization in both healthy subjects and schizophrenia patients [58,63]. Our own findings add to these results from previous studies by suggesting that MET RNA variations may entail structural changes including aberrant structural asymmetry of Broca's subareas in schizophrenia, which impair neurocognitive functions, possibly via altered functional connectivity.

A similar gene–brain structure–symptom relationship is less evident for the *SIRT1* gene, which is upregulated in left area 45, where we found decreased volume and a linear negative relationship with the negative symptom dimension in patients. *SIRT1* encodes a member of the sirtuin family of proteins, which substantially contributes to the regulation of cellular metabolism in response to stressful conditions [64], of the circadian rhythms, and of dopamine pathways [65,66]. A low mRNA expression level of *SIRT1* has especially been documented in schizophrenia patients with

depressive symptoms [67,68]. It has therefore been concluded that genetic variants of *SIRT1* make schizophrenia patients more prone to depressive symptoms and that the corresponding SNP might be a biomarker of depression in schizophrenia [69]. That the gray matter reduction that we found in left area 45 was related to the negative subtype might thus be due to a pathophysiological overlap and association with depressive symptoms [70,71]. This explanation seems particularly reasonable given its consistent volume reduction not only in schizophrenia but also major depressive and bipolar disorder [72].

Taken together, we found a link between altered asymmetry of Broca's subareas and the degree of specific psychopathology and showed that gray matter reduction of left area 44 is associated with negative symptoms, while cognitive symptoms are linked to gray matter loss in right area 45. Subregional reductions in gray matter and in asymmetry may hence entail alterations in brain function, which in turn involve altered behavior, i.e., symptoms. Gene expression analyses indicated that variations of *MET* might underlie these structural changes and thus corresponding symptom dimensions. These specific morphometry–gene associations were identified using an indirect approach. We anticipate our findings to be a starting point for more direct genetic analyses of brain tissue in these areas. For example, RNA expression differences between patients and controls could be tested in transcriptome analyses of post-mortem brain tissue, including prior individual cytoarchitectonic delineation of areae 44/45. Our results substantiate previous findings suggesting a critical role for Broca's area (and its homolog) in the psychopathology of schizophrenia by establishing a relationship between genetics, neuroanatomy, and symptom on the subregional level.

Methods

Participants

The sample comprised 478 individuals from seven sites. A total of 236 patients (68 female, mean age = 33.8 ± 11.0 years, range 18–66 years) diagnosed with schizophrenia according to the DSM-IV as well as 242 age- and sex-matched healthy controls (77 female, mean age = 33.7 ± 11.1 years, range 19–65 years) from seven independent medical centers located in the USA, Europe and Singapore were included. All participants provided written informed consent in accordance with the Declaration of Helsinki. Experiments have been approved by the local ethics committees at the University of new Mexico (USA), the University of Regensburg (Germany), Georg August University Göttingen (Germany), University Medical Center Groningen (Netherlands), University Medical Center Utrecht (Netherlands), Institute of Mental Health and the National Neuroscience Institute (Singapore). Detailed information on participants' characteristics (and on characteristics of an independent replication sample) is provided in Supplementary Methods.

Clinical assessment

Psychopathological symptoms of schizophrenia were assessed using the Positive and Negative Syndrome Scale (PANSS) [73]. According to a recent machine learning based factorization analysis (orthogonal projective non-negative matrix factorization) in two large multi-site schizophrenia samples [74], PANSS items were grouped into four stable and generalizable data-driven symptom dimensions: positive, negative, cognitive, and affective. For each patient, a score reflecting each symptom dimension was computed by means of the "Dimensions and Clustering Tool for assessing schizophrenia Symptomatology" (DCTS), where higher scores indicate higher symptom severity.

Image acquisition, preprocessing and region-based morphometry

High-resolution T1-weighted structural imaging was performed for each site (Supplementary Table 2). Structural MRI scans were preprocessed using the Computational Anatomy Toolbox (CAT) as an extension to the SPM12 software for voxel-based morphometry analysis. Preprocessing steps include segmentation into gray matter, white matter, and cerebrospinal fluid as well as spatial normalization into Montreal Neurological Institute space. We assessed Broca's region and its right homolog as regions of interest using the Julich Brain Atlas, which is based on an observer-independent cyto-architectonic mapping approach [75,76]. To estimate the mean value of local gray matter volume of their subregions, we capitalized on the cytoarchitectonically defined maximum probability maps of the Julich Brain Atlas as derived from ten histologically and computationally analyzed postmortem brains [25]. These maps describe the inter-individual variability of a particular cortical or subcortical structure to be found at each voxel position of a reference brain space, reflected by a probability

value for each voxel. We selected the maps of area 44 (doi: 10.25493/K06P-R2S) (from both hemispheres), together covering what is traditionally considered Broca's area (and its homolog) (Fig. 1A). Total intracranial volume (TIV) was estimated for each subject and used as a covariate in all subsequent analyses.

Statistical analysis

Region-based morphometry analysis of gray matter volume

We employed a two-factorial repeated measures ANCOVA with hemisphere (left/right) as well as cytoarchitectonic area (44/45) as within-subject factors including TIV as well as site/scanner as covariates and with group as between-subject factor (patients/controls). The statistical significance level for post hoc t-tests was set at p < 0.05 (Bonferroni-corrected). ANCOVA effect sizes were estimated as partial η^2 values. To estimate the achieved power for the post hoc t-tests, we computed Cohen's d employing the free software package $\underline{G^*Power}$ [77]. The relationship between gray matter volume and the severity of the four psychotic symptom dimensions was assessed by calculating non-parametric partial rank correlations (including TIV as well as site/scanner as covariates) with statistical significance level at p < 0.05 (Bonferroni-corrected).

Functional characterization

Functional characterization intends to link topographically defined brain regions with corresponding psychological processes by testing which kind of experiments are most likely to activate a given region. To functionally characterize the regions exhibiting altered morphology related to one of the symptom dimensions, we made use of the BrainMap database that currently contains ≈8000 experiments in healthy adults (experiments investigating age, gender, disease, or drug effects excluded). BrainMap meta-data provide information on behavioral domain and paradigm class of each neuroimaging experiment included in the database. Behavioral domains describe the mental processes isolated by the statistical contrasts [78] and comprise the main categories action, cognition, emotion, interoception, and perception, as well as their subcategories. Paradigm classes specify the task employed in the corresponding neuroimaging studies (see www.brainmap.org for the complete BrainMap taxonomy). To describe the functional roles of the candidate regions, we used a reverse inference approach, which tests the probability of a mental process being present, given knowledge that a particular brain region is activated [79,80]. More precisely, the functional profile of a region was determined by overrepresentation of mental processes (i.e., behavioral domains and paradigm classes) in the experiments activating the respective cluster relative to the entire BrainMap database using a binomial test [79,80]. The significance threshold was set to a liberal threshold of p < 0.05 to draw a differentiated picture that the morphology-symptom relationship observed in our patients corresponds with an activity-function relationship in healthy subjects. This approach provides an objective and quantitative attribution of mental functions to brain regions in contrast to commonly used qualitative and subjective interpretation of foci in neuroimaging.

Asymmetry of gray matter volume

Asymmetry of areas 44 and 45 in each individual was quantified on basis of the Asymmetry Index (AI), which is a common measure of structural brain asymmetry and defined as: (left - right volume) / (left + right volume) [range -1 to +1] [81,82]. Positive values hence indicate leftward asymmetry, while negative values indicate rightward asymmetry. A two-tailed two-sample *t*-test was performed to evaluate differences in asymmetry of areas 44 and 45 between the group of patients and healthy controls.

Gene expression analysis

Differences of regional gene expression was analyzed using <u>JuGEx</u> [83], a tool that combines mRNA expression data of the Allen Human Brain Atlas [84,85] with the three-dimensional cytoarchitectonic probability maps from the Julich Brain Atlas [25] to statistically compare gene expression levels between two areas in a common reference brain space. According to the notion that the genetic variance associated with the evolution of hemispheric dominance for language carries with it the hazard of the symptoms of schizophrenia [5,8], we focused on genes implicated in both schizophrenia and evolution of the human faculty of language. Therefore, we did not just select Psychiatric Genomic Consortium (PGC) vulnerability genes for schizophrenia [86,87]. Rather, the selection of genes was guided by Murphy and Benítez-Burraco [28] who identified candidate genes for schizophrenia that are overrepresented in the group of genes related to human language ability. We selected the 20 reported genes that i) were identified through GWAS and ii) are suggested to be involved in the evolution of language abilities (due to our focus on Broca's region and its right homolog) (Supplementary Table 3). To find evidence for a regional specificity of the gene activity in left and right areas 44 and 45, we compared their mRNA expression levels with those of frontal lobe88]). That is, we selected the cytoarchitectonic subregions of the left and right premotor cortex (areas 6d1 (doi: 10.25493/KSY8-H3F), 6d2 (doi: 10.25493/WJQ5-HWC), 6d3 (doi: doi.org/10.25493/D41S-AG7) and merged them to a single probabilistic map. For downloading expression data from the Allen Human Brain Atlas, we set a threshold of 20% to ensure an inclusion of multiple tissue samples and a proper covering of the anatomically delineated expression variability within the investigated areas. To compare the gene expression between Broca's region (and its homolog) and the premotor subregions, relative expression values (z-score-normalized) were used as dependent variables. The statistical analysis was performed using "all-probes mode", which averages z-scores of all microarray probes available from the Allen data for a specific gene. Statistical analysis of expression was calculated with the z-scores thus summarized using a non-parametric *n*-way ANOVA with 10,000 permutations. The resulting p-values were corrected using the family-wise error (FWE) correction based on the

total number of parallelly analyzed genes (n = 20). A gene was considered as significantly upregulated (i.e., active) if the regionally specific z-score of a gene implied a higher gene expression in one region compared to another ($p_{\text{FWE}} < 0.05$). To evaluate the methodological robustness as well as the biological specificity of our findings, we performed a control analysis. Here, we compared Broca's subregions and the premotor cortex (as defined above) with an independent gene set comprising 14 genes from GWAS of eye, hair, and skin coloration ("color genes") (Supplementary Table 4).

Data availability

Data of COBRE were obtained from the SchizConnect, a publicly available website (http://www.schizconnect.org/documentation#by project). The COBRE dataset was downloaded from the Center for Biomedical Research Excellence in Brain Function and Mental Illness (COBRE) (https://coins.trendscenter.org/). Data from the other datasets are not publicly available for download, but access requests can be made to the respective study investigators: Aachen—B. Derntl (oliver.gruber@med.uni-heidel-(birgit.derntl@med.uni-tuebingen.de); Göttingen—O. Gruber berg.de); Groningen—André Aleman (a.aleman@umcg.nl); Utrecht—I.E. Sommer (i.e.c.sommer@umcg.nl), Regensburg—corresponding author: T.B. Poeppl; Singapore—J.H. Zhou (helen.zhou@nus.edu.sg). Requests for raw and analyzed data can be made to the corresponding author T.B. Poeppl and will be promptly reviewed by the Ethics Committee at the University of Regensburg to verify whether the request is subject to any intellectual property or confidentiality obligations. The Jülich Brain Atlas is accessible at https://julich-brain-atlas.de, the BrainMap database at http://www.brainmap.org/.

Code availability

The "Dimensions and Clustering Tool for assessing schizophrenia Symptomatology" (DCTS) is available at http://webtools.inm7.de/sczDCTS/, the Computational Anatomy Toolbox (CAT) at https://www.fil.ion.ucl.ac.uk/spm/soft-ware/spm12/, G*Power software at https://www.fz-juel-ich.de/de/inm/inm-1/leistungen/tools-services-und-forschungsdaten/jugex.

Acknowledgements

This research project is supported by a grant from the START-Program of the Faculty of Medicine of the RWTH Aachen University (37/20; funded by the North Rhine-Westphalian Ministry of Culture and Science).

J.H.Z. was supported by Yong Loo Lin School of Medicine, National University of Singapore.

Author contributions

T.B.P., S.Z. and K.S. designed the study; S.B.E. gave conceptual advice. A.A., T.B., B.D., E.F., T.F., P.F.-C., M.Á.G.-L., O.G., G.H., R.J., L.K., P.M.K., D.M., M.L., B.L., E.P.-C., J.P., M.S., K.S., J.S.-V., I.E.S., J.H.Z. and T.B.P. contributed data. S.Z. conducted the analyses under supervision by K.S. and T.B.P. F.H. organized and preprocessed data of the replication sample. J.A.C. and S.B.E.

provided the functional characterization. S.B., D.I.P. and T.W.M. advised on the gene expression analyses. S.Z. and T.B.P. wrote the manuscript. S.B., D.I.P., S.H., T.W.M. and S.B.E. discussed the results and implications. All authors commented on the manuscript at all stages.

Competing interests

The authors declare no competing interests.

Tables

Table 1. Statistical comparisons of gray matter volume for single cytoarchitectonic areas.

		•			
	SCZ (n = 236)	HC (n = 242)			
	Mean (SD)	Mean (SD)	t	p	Cohen's d
Left hemisphere					
44	4.1 (0.8)	4.4 (0.6)	5.352	< 0.001	0.491
45	2.0 (0.4)	2.2 (0.3)	5.908	< 0.001	0.540
Right hemisphere					
44	2.0 (0.4)	2.1 (0.4)	3.245	0.001	0.287
45	3.0 (0.6)	3.2 (0.5)	5.075	< 0.001	0.464

Two-sided *t*-tests indicated significantly decreased gray matter volume [ml] in all four areas. Multiple comparisons were accounted for with Bonferroni correction.

Table 2. Correlation between regional gray matter volume and symptom dimensions in patients.

	Left Hemisphere		Right Hemisphere	
	44	45	44	45
Positive dimension	-0.062	-0.021	-0.077	-0.138
Negative dimension	-0.177***	-0.157**	-0.112	-0.131
Cognitive dimension	-0.146	-0.138	-0.080	-0.150*
Affective dimension	-0.143	-0.077	-0.098	-0.106

Non-parametric partial rank correlation analyses (two-sided) indicated a significant negative correlation between severity of negative symptoms and gray matter volume of left areas 44/45 as well as between severity of cognitive symptoms with gray matter volume of right area 45.

Numbers represent Spearman's ϱ . Multiple comparisons were accounted for with Bonferroni correction. p = 0.011; p = 0.008, p = 0.008, p = 0.008.

SCZ = schizophrenia patients; HC = healthy controls

Figure Legends/Captions

- **Fig. 1. Volumetric differences in areas 44 and 45 between patients and healthy controls. (A)** Shape and location of Broca's cytoarchitectonic subregions (and homologs) in the left and right hemispheres. Areas 44 (red) and 45 (green) are defined according to probabilistic maps of the Julich Brain Atlas. **(B)** Two-sided t-tests indicated significantly decreased gray matter volume of all areas in patients (n = 236) as compared to controls (n = 242). Multiple comparisons were accounted for with Bonferroni correction. The boxes indicate the 75th (upper horizontal line), median (middle horizontal line) and 25th (lower horizontal line) percentiles of the distribution; the whiskers indicate the range of data.
- Fig. 2. Association between gray matter morphology and symptom dimensions. Non-parametric partial rank correlation analyses (two-sided) showed significant associations of negative symptoms with left area 44 (A) as well as left area 45 (B) and between right area 45 and cognitive symptoms (C). Multiple comparisons were accounted for with Bonferroni correction.
- **Fig. 3. 3D visualization of the regional specification analysis.** Gene expression was compared between (Broca's) areas 44/45 (red) and control regions (premotor cortex; blue). Two of the candidate genes showed a significant differential expression: *MET* was upregulated in areas 44 and 45 of the left hemisphere and in area 45 of the right hemisphere; *SIRT1* was upregulated in left area 45 only. Analyzed tissue samples are represented in spheres, with expression levels represented by z-scores with minimum values indicated in pink and maximum values in green color.

References

- 1. Hilker, R., et al. Heritability of schizophrenia and schizophrenia spectrum based on the nationwide danish twin register. *Biol Psychiatry* **83**, 492-498 (2018).
- 2. Heim, S., Dehmer, M. & Berger-Tunkel, M. Impairments of language and communication in schizophrenia. *Nervenarzt* **90**, 485-489 (2019).
- 3. Covington, M.A., *et al.* Schizophrenia and the structure of language: the linguist's view. *Schizophr Res* **77**, 85-98 (2005).
- 4. Mitchell, R.L. & Crow, T.J. Right hemisphere language functions and schizophrenia: the forgotten hemisphere? *Brain* **128**, 963-978 (2005).
- Crow, T.J. Schizophrenia as failure of hemispheric dominance for language. *Trends Neurosci* 339-343 (1997).
- 6. Marini, A., et al. The language of schizophrenia: an analysis of micro and macrolinguistic abilities and their neuropsychological correlates. *Schizophr Res* **105**, 144-155 (2008).
- 7. Kuperberg, G.R. Language in schizophrenia Part 1: an Introduction. *Lang Linguist Compass* **4**, 576-589 (2010).
- 8. Angrilli, A., et al. Schizophrenia as failure of left hemispheric dominance for the phonological component of language. *PLoS One* **4**, e4507 (2009).
- 9. Sans-Sansa, B., et al. Association of formal thought disorder in schizophrenia with structural brain abnormalities in language-related cortical regions. *Schizophr Res* **146**, 308-313 (2013).
- 10. Rimol, L.M., et al. Cortical volume, surface area, and thickness in schizophrenia and bipolar disorder. *Biol Psychiatry* **71**, 552-560 (2012).

- 11. Wisco, J.J., *et al.* Abnormal cortical folding patterns within Broca's area in schizophrenia: evidence from structural MRI. *Schizophr Res* **94**, 317-327 (2007).
- 12. Jung, S., Lee, A., Bang, M. & Lee, S.H. Gray matter abnormalities in language processing areas and their associations with verbal ability and positive symptoms in first-episode patients with schizophrenia spectrum psychosis. *Neuroimage Clin* **24**, 102022 (2019).
- 13. Jung, W.H., *et al.* Regional brain atrophy and functional disconnection in Broca's area in individuals at ultra-high risk for psychosis and schizophrenia. *PLoS One* **7**, e51975 (2012).
- 14. Fedorenko, E., Duncan, J. & Kanwisher, N. Language-selective and domain-general regions lie side by side within Broca's area. *Curr Biol* **22**, 2059-2062 (2012).
- 15. Koutsouleris, N., *et al.* Structural correlates of psychopathological symptom dimensions in schizophrenia: a voxel-based morphometric study. *Neuroimage* **39**, 1600-1612 (2008).
- 16. Cavelti, M., Kircher, T., Nagels, A., Strik, W. & Homan, P. Is formal thought disorder in schizophrenia related to structural and functional aberrations in the language network? A systematic review of neuroimaging findings. *Schizophr Res* 199, 2-16 (2018).
- 17. Gaser, C., Nenadic, I., Volz, H.P., Büchel, C. & Sauer, H. Neuroanatomy of "hearing voices": a frontotemporal brain structural abnormality associated with auditory hallucinations in schizophrenia. *Cereb Cortex* **14**, 91-96 (2004).
- 18. Suga, M., et al. Reduced gray matter volume of Brodmann's Area 45 is associated with severe psychotic symptoms in patients with schizophrenia. Eur Arch Psychiatry Clin Neurosci 260, 465-473 (2010).
- 19. Palaniyappan, L., et al. Structural correlates of formal thought disorder in schizophrenia: An ultra-high field multivariate morphometry study. *Schizophr Res* **168**, 305-312 (2015).

- 20. Berlim, M.T., Mattevi, B.S., Belmonte-de-Abreu, P. & Crow, T.J. The etiology of schizophrenia and the origin of language: overview of a theory. *Compr Psychiatry* **44**, 7-14 (2003).
- 21. Kawasaki, Y., et al. Anomalous cerebral asymmetry in patients with schizophrenia demonstrated by voxel-based morphometry. *Biol Psychiatry* **63**, 793-800 (2008).
- 22. Shivakumar, V., Sreeraj, V.S., Kalmady, S.V., Gangadhar, B.N. & Venkatasubramanian, G. pars triangularis volume asymmetry and schneiderian first rank symptoms in antipsychotic-naïve schizophrenia. *Clin Psychopharmacol Neurosci* **19**, 507-513 (2021).
- 23. Keller, S.S., Crow, T., Foundas, A., Amunts, K. & Roberts, N. Broca's area: nomenclature, anatomy, typology and asymmetry. *Brain Lang* **109**, 29-48 (2009).
- 24. Brugger, S.P. & Howes, O.D. Heterogeneity and homogeneity of regional brain structure in schizophrenia: a meta-analysis. *JAMA Psychiatry* **74**, 1104-1111 (2017).
- 25. Amunts, K., Mohlberg, H., Bludau, S. & Zilles, K. Julich-Brain: A 3D probabilistic atlas of the human brain's cytoarchitecture. *Science* **369**, 988-992 (2020).
- 26. Ripke, S., et al. Biological insights from 108 schizophrenia-associated genetic loci. *Nature* **511**, 421-427 (2014).
- 27. Pardiñas, A.F., *et al.* Common schizophrenia alleles are enriched in mutation-intolerant genes and in regions under strong background selection. *Nat Genet* **50**, 381-389 (2018).
- 28. Murphy, E. & Benítez-Burraco, A. Bridging the gap between genes and language deficits in schizophrenia: An oscillopathic approach. *Front Hum Neurosci* **10**, 422 (2016).
- Stefaniak, J.D., Alyahya, R.S.W. & Lambon Ralph, M.A. Language networks in aphasia and health: A 1000 participant activation likelihood estimation meta-analysis. *Neuroimage* 233, 117960 (2021).

- 30. Jackson, R.L. The neural correlates of semantic control revisited. *Neuroimage* **224**, 117444 (2021).
- 31. Hartwigsen, G., Neef, N.E., Camilleri, J.A., Margulies, D.S. & Eickhoff, S.B. Functional segregation of the right inferior frontal gyrus: evidence from coactivation-based parcellation.

 Cereb Cortex 29, 1532-1546 (2019).
- 32. Bzdok, D., *et al.* Parsing the neural correlates of moral cognition: ALE meta-analysis on morality, theory of mind, and empathy. *Brain Struct Funct* **217**, 783-796 (2012).
- 33. Chen, J., et al. Intrinsic connectivity patterns of task-defined brain networks allow individual prediction of cognitive symptom dimension of schizophrenia and are linked to molecular architecture. *Biol Psychiatry* **89**, 308-319 (2021).
- 34. Gavilán Ibáñez, J.M. & García-Albea Ristol, J.E. Theory of mind and language comprehension in schizophrenia. *Psicothema* **25**, 440-445 (2013).
- 35. Allen, P., et al. Neuroimaging auditory hallucinations in schizophrenia: from neuroanatomy to neurochemistry and beyond. *Schizophr Bull* **38**, 695-703 (2012).
- 36. Ćurčić-Blake, B., et al. Interaction of language, auditory and memory brain networks in auditory verbal hallucinations. *Prog Neurobiol* **148**, 1-20 (2017).
- 37. Romeo, Z. & Spironelli, C. Hearing voices in the head: Two meta-analyses on structural correlates of auditory hallucinations in schizophrenia. *Neuroimage Clin* **36**, 103241 (2022).
- 38. Modinos, G., et al. Neuroanatomy of auditory verbal hallucinations in schizophrenia: a quantitative meta-analysis of voxel-based morphometry studies. *Cortex* **49**, 1046-1055 (2013).
- 39. Palaniyappan, L., Balain, V., Radua, J. & Liddle, P.F. Structural correlates of auditory hallucinations in schizophrenia: a meta-analysis. *Schizophr Res* **137**, 169-173 (2012).

- 40. Jardri, R., Pouchet, A., Pins, D. & Thomas, P. Cortical activations during auditory verbal hallucinations in schizophrenia: a coordinate-based meta-analysis. *Am J Psychiatry* **168**, 73-81 (2011).
- 41. Zmigrod, L., Garrison, J.R., Carr, J. & Simons, J.S. The neural mechanisms of hallucinations:

 A quantitative meta-analysis of neuroimaging studies. *Neurosci Biobehav Rev* **69**, 113-123 (2016).
- 42. Fovet, T., et al. Decoding Activity in Broca's Area Predicts the Occurrence of Auditory Hallucinations Across Subjects. *Biol Psychiatry* **91**, 194-201 (2022).
- 43. Sommer, I.E., et al. Auditory verbal hallucinations predominantly activate the right inferior frontal area. *Brain* **131**, 3169-3177 (2008).
- 44. Clos, M., Amunts, K., Laird, A.R., Fox, P.T. & Eickhoff, S.B. Tackling the multifunctional nature of Broca's region meta-analytically: co-activation-based parcellation of area 44. *Neuroimage* 83, 174-188 (2013).
- 45. Adolphs, R., Damasio, H., Tranel, D., Cooper, G. & Damasio, A.R. A role for somatosensory cortices in the visual recognition of emotion as revealed by three-dimensional lesion mapping. *J Neurosci* **20**, 2683-2690 (2000).
- de la Rosa, S., Schillinger, F.L., Bülthoff, H.H., Schultz, J. & Uludag, K. fMRI adaptation between action observation and action execution reveals cortical areas with mirror neuron properties in human BA 44/45. *Front Hum Neurosci* **10**, 78 (2016).
- 47. Rizzolatti, G. & Fabbri-Destro, M. Mirror neurons: from discovery to autism. *Exp Brain Res* **200**, 223-237 (2010).
- 48. Bonini, L., Rotunno, C., Arcuri, E. & Gallese, V. Mirror neurons 30 years later: implications and applications. *Trends Cogn Sci* **26**, 767-781 (2022).

- 49. Gallese, V. & Goldman, A. Mirror neurons and the simulation theory of mind-reading. *Trends Cogn Sci* **2**, 493-501 (1998).
- 50. Mehta, U.M., *et al.* Mirror neuron dysfunction in schizophrenia and its functional implications: a systematic review. *Schizophr Res* **160**, 9-19 (2014).
- 51. Brüne, M. "Theory of mind" in schizophrenia: a review of the literature. *Schizophr Bull* **31**, 21-42 (2005).
- 52. Tseng, C.E., *et al.* Altered cortical structures and tract integrity of the mirror neuron system in association with symptoms of schizophrenia. *Psychiatry Res* **231**, 286-291 (2015).
- 53. Schilbach, L., *et al.* Differential patterns of dysconnectivity in mirror neuron and mentalizing networks in schizophrenia. *Schizophr Bull* **42**, 1135-1148 (2016).
- 54. Lee, J.S., Chun, J.W., Yoon, S.Y., Park, H.J. & Kim, J.J. Involvement of the mirror neuron system in blunted affect in schizophrenia. *Schizophr Res* **152**, 268-274 (2014).
- 55. Lane, R.D.N., L. (Eds.). Cognitive neuroscience of emotion, (Oxford University Press, 2000).
- 56. Robinson, D.R., Wu, Y.M. & Lin, S.F. The protein tyrosine kinase family of the human genome. *Oncogene* **19**, 5548-5557 (2000).
- 57. Mukamel, Z., et al. Regulation of MET by FOXP2, genes implicated in higher cognitive dysfunction and autism risk. *J Neurosci* **31**, 11437-11442 (2011).
- 58. Ocklenburg, S., *et al.* FOXP2 variation modulates functional hemispheric asymmetries for speech perception. *Brain Lang* **126**, 279-284 (2013).
- 59. Sanjuán, J., et al. Association between FOXP2 polymorphisms and schizophrenia with auditory hallucinations. *Psychiatr Genet* **16**, 67-72 (2006).

- 60. McCarthy-Jones, S., et al. Preliminary evidence of an interaction between the FOXP2 gene and childhood emotional abuse predicting likelihood of auditory verbal hallucinations in schizophrenia. *J Psychiatr Res* **50**, 66-72 (2014).
- 61. Burdick, K.E., DeRosse, P., Kane, J.M., Lencz, T. & Malhotra, A.K. Association of genetic variation in the MET proto-oncogene with schizophrenia and general cognitive ability. *Am J Psychiatry* **167**, 436-443 (2010).
- 62. Du, J., et al. The genetic determinants of language network dysconnectivity in drug-naïve early stage schizophrenia. NPJ Schizophr 7, 18 (2021).
- 63. Pinel, P., et al. Genetic variants of FOXP2 and KIAA0319/TTRAP/THEM2 locus are associated with altered brain activation in distinct language-related regions. *J Neurosci* 32, 817-825 (2012).
- 64. Vassilopoulos, A., Fritz, K.S., Petersen, D.R. & Gius, D. The human sirtuin family: evolutionary divergences and functions. *Hum Genomics* **5**, 485-496 (2011).
- 65. Kishi, T., et al. SIRT1 gene, schizophrenia and bipolar disorder in the Japanese population: an association study. *Genes Brain Behav* **10**, 257-263 (2011).
- 66. Wang, Y., et al. Association between Silent Information Regulator 1 (SIRT1) gene polymorphisms and schizophrenia in a Chinese Han population. *Psychiatry Res* **225**, 744-745 (2015).
- 67. Fang, X., Chen, Y., Wang, Y., Ren, J. & Zhang, C. Depressive symptoms in schizophrenia patients: A possible relationship between SIRT1 and BDNF. *Prog Neuropsychopharmacol Biol Psychiatry* **95**, 109673 (2019).
- 68. Luo, X.J. & Zhang, C. Down-regulation of SIRT1 gene expression in major depressive disorder. *Am J Psychiatry* **173**, 1046 (2016).

- 69. Wang, D., et al. A Comprehensive analysis of the effect of SIRT1 variation on the risk of schizophrenia and depressive symptoms. *Front Genet* **11**, 832 (2020).
- 70. Krynicki, C.R., Upthegrove, R., Deakin, J.F.W. & Barnes, T.R.E. The relationship between negative symptoms and depression in schizophrenia: a systematic review. *Acta Psychiatr Scand* **137**, 380-390 (2018).
- 71. Guessoum, S.B., Le Strat, Y., Dubertret, C. & Mallet, J. A transnosographic approach of negative symptoms pathophysiology in schizophrenia and depressive disorders. *Prog Neuropsychopharmacol Biol Psychiatry* **99**, 109862 (2020).
- 72. Brosch, K., et al. Reduced hippocampal gray matter volume is a common feature of patients with major depression, bipolar disorder, and schizophrenia spectrum disorders. *Mol Psychiatry* (2022).
- 73. Kay, S.R., Fiszbein, A. & Opler, L.A. The positive and negative syndrome scale (PANSS) for schizophrenia. *Schizophr Bull* **13**, 261-276 (1987).
- 74. Chen, J., et al. Neurobiological divergence of the positive and negative schizophrenia subtypes identified on a new factor structure of psychopathology using non-negative factorization: An international machine learning study. *Biol Psychiatry* 87, 282-293 (2020).
- 75. Amunts, K., et al. Broca's region revisited: cytoarchitecture and intersubject variability. *J*Comp Neurol **412**, 319-341 (1999).
- 76. Amunts, K., Schleicher, A. & Zilles, K. Outstanding language competence and cytoarchitecture in Broca's speech region. *Brain Lang* **89**, 346-353 (2004).
- 77. Faul, F., Erdfelder, E., Lang, A.G. & Buchner, A. G*Power 3: a flexible statistical power analysis program for the social, behavioral, and biomedical sciences. *Behav Res Methods* **39**, 175-191 (2007).

- 78. Fox, P.T., *et al.* BrainMap taxonomy of experimental design: description and evaluation. *Hum Brain Mapp* **25**, 185-198 (2005).
- 79. Poeppl, T.B., *et al.* Imbalance in subregional connectivity of the right temporoparietal junction in major depression. *Hum Brain Mapp* **37**, 2931-2942 (2016).
- 80. Poeppl, T.B., *et al.* A view behind the mask of sanity: meta-analysis of aberrant brain activity in psychopaths. *Mol Psychiatry* **24**, 463-470 (2019).
- 81. de Kovel, C.G.F., *et al.* No alterations of brain structural asymmetry in major depressive disorder: an ENIGMA consortium analysis. *Am J Psychiatry* **176**, 1039-1049 (2019).
- 82. Okada, N., et al. Abnormal asymmetries in subcortical brain volume in schizophrenia. *Mol Psychiatry* **21**, 1460-1466 (2016).
- 83. Bludau, S., et al. Integration of transcriptomic and cytoarchitectonic data implicates a role for MAOA and TAC1 in the limbic-cortical network. *Brain Struct Funct* **223**, 2335-2342 (2018).
- 84. Hawrylycz, M.J., *et al.* An anatomically comprehensive atlas of the adult human brain transcriptome. *Nature* **489**, 391-399 (2012).
- 85. Hawrylycz, M., *et al.* Canonical genetic signatures of the adult human brain. *Nat Neurosci* **18**, 1832-1844 (2015).
- 86. Kong, X.Z., et al. Gene Expression Correlates of the Cortical Network Underlying Sentence Processing. *Neurobiol Lang (Camb)* **1**, 77-103 (2020).
- 87. Romme, I.A., de Reus, M.A., Ophoff, R.A., Kahn, R.S. & van den Heuvel, M.P. Connectome Disconnectivity and Cortical Gene Expression in Patients With Schizophrenia. *Biol Psychiatry* 81, 495-502 (2017).

88. Unger, N., et al. Identification of phonology-related genes and functional characterization of Broca's and Wernicke's regions in language and learning disorders. Front Neurosci 15, 680762 (2021).

Supplementary Information

Supplementary Methods

Experimental sample

The sample comprised 478 individuals in total (see Supplementary Table 1). Patients and healthy controls from seven independent medical centers located in the USA, Europe and Singapore were included: 1) a dataset of 66 patients and 55 healthy controls retrieved from the Mind Research Network Center of Biomedical Research Excellence (COBRE) funded by the National Institutes of Health; these data are shared via the Mind Research Network's collaborative informatics and neuroimaging suite (COINS) [detailed information on the data collection procedure is provided in the publication by Aine et al.[1]]; 2) a dataset of 23 patients and 23 controls recruited at the University of Regensburg between 2008 and 2010 (Regensburg 1) [further information on the data collection procedure is reported elsewhere [2]]; another dataset of 19 patients and 20 controls recruited at the University of Regensburg between 2014 and 2016 (Regensburg 2); 3) a dataset comprising 12 patients and 11 healthy controls recruited at RWTH Aachen University (Aachen sample) [3]; 4) a dataset of 26 patients and 27 healthy controls recruited at the University Medical Center Göttingen (Göttingen sample) [4]; 5) a dataset of 15 patients and 19 healthy controls recruited at the Medical University Center Groningen (Groningen sample) [5]; 6) a dataset of 7 patients and 10 healthy controls recruited at the University Medical University Center Utrecht (Utrecht sample) [6]; 7) another dataset of 68 patients and 77 healthy controls recruited at the Institute of Mental Health in Singapore (Singapore sample) [7].

Replication sample

An independent replication sample comprised 249 individuals in total. We included a total of 136 patients (37 female, mean age = 37.3 ± 10.8 years, range 18–66 years) diagnosed with schizophrenia according to the DSM-IV as well as 113 age- and sex-matched healthy controls (40 female, mean age = 35.1 ± 11.6 years, range 19–64 years) from four independent medical centers located in Europe: 1) a dataset of 20 patients and 20 controls recruited from the Department of Psychiatry, Klinikum rechts der Isar, Technische Universität München [8]; 2) a dataset of 16 patients and 16 controls recruited at the Department of Psychiatry, Fontan Hospital, CHU Lille, Universitaire de Lille [9]; 3) a dataset of 54 patients recruited at the University of Regensburg and being enrolled in a multicenter center trial between 2007 and 2011 [10,11], and 53 controls who were recruited simultaneously at University of Regensburg; 4) another dataset of 46 patients and 24 controls recruited from four psychiatric hospitals in Barcelona (Benitio Menni CASM, Hospital Sagrat Cor de Matrorell, Sant Rafael Hospital, Hospital de la Mercé) [12]. All participants provided written informed consent in accordance with the Declaration of Helsinki. Experiments have been approved by the local ethics committees.

Supplementary Results

Gray matter volume in the replication sample

We first used region-based morphometry to test for gray matter differences between patients and comparison subjects within individual left and right cytoarchitectonic areas 44 and 45 (i.e., four regions). ANCOVA revealed only a main effect of group ($F_{1,245} = 26.136$; p < 0.001, $\eta_p^2 = 0.096$). There was a significant interaction group × hemisphere ($F_{1,245} = 18.113$; p < 0.001, $\eta_p^2 = 0.069$). Also, the group × cytoarchitectonic area × hemisphere ($F_{1,245} = 19.267$; p < 0.001, $\eta_p^2 = 0.073$) interaction yielded statistical significance. We then conducted post hoc t-tests to compare group means. These revealed significantly reduced gray matter volume of all four areas in patients. The strongest effect of group was found for left area 44 ($t_{247} = 6.370$; p < 0.001, d = 0.819). For right area 44 ($t_{247} = 4.743$; p < 0.001, d = 0.608) and left area 45 ($t_{247} = 3.705$; p < 0.001, d = 0.472), small to medium effect sizes were observed. Right area 45 showed the smallest effect ($t_{247} = 3.271$; p = 0.001, d = 0.418).

Supplementary Tables

Supplementary Table 1. Clinical and demographic characteristics of patients with schizophrenia and controls

SCZ (n = 236)	HC (n = 242)
Mean (SD)	Mean (SD)
33.7 (11.0)	33.7 (11.1)
168/68	165/77
9.2 (10.4)	
14.8 (5.4)	
14.0 (6.6)	
28.3 (10.4)	
57.1 (19.9)	
247.9 (292.9)	
	Mean (SD) 33.7 (11.0) 168/68 9.2 (10.4) 14.8 (5.4) 14.0 (6.6) 28.3 (10.4) 57.1 (19.9)

SCZ = schizophrenia patients; HC = healthy controls

Supplementary Table 2. T1-weighted structural MRI scanning parameters for each site

Site	Scanner	TR (ms)	TE (ms)	FA (°)	No. Slices	Slice Thickness (mm)	Voxel Size (mm³)
COBRE	Siemens TrioTim 3T ¹	2,530	[1.64–9.08]	7	176	1	1 x 1 x1
Regensburg 1	Siemens MAGNETOM Sonata 1.5T	1,880	3.93	15	176	1	0.977 × 0.977 × 1
Regensburg 2	Siemens MAGNETOM Aera 1.5T	2,060	5.99	15	160	1	1 × 1 ×1
Aachen	Siemens TrioTim 3T	2,300	3.03	9	176	1	1 × 1 ×1
Göttingen	Siemens MAGNETOM Trio 3T	11.9	4.42	15	176	1	1 × 1 ×1
Groningen	Philips Intera 3T	25	4.6	30	160	1	1 × 1 ×1
Utrecht	Philips Achieva 3T	9.86	4.59	n.a.	160	1	0.875 × 0.875 ×1
Singapore	Siemens TrioTim 3T	8,400	3.8	8	180	0.9	1 x 1 x1

TR = repetition time; TE = echo time; FA = flip angle ¹a multi-echo MPRAGE sequence with 5 TE's

Supplementary Table 3. Candidate genes for schizophrenia that are overrepresented in the group of genes that are candidates for language readiness according to Murphy & Benitez-Burraco (2016)

Gene ¹	Gene name	HGNC ID ²	ENTREZ ID ³	ENSEMBL ID4
AKT1	AKT serine/threonine kinase 1	391	207	ENSG00000142208
CDC42	cell division cycle 42	1736	998	ENSG00000070831
CNTNAP2	contactin associated protein-like 2	13830	26047	ENSG00000174469
DISC1	disrupted in schizophrenia 1	2888	27185	ENSG00000162946
ELAVL2	ELAV like neuron-specific RNA binding protein 2	3313	1993	ENSG00000107105
ERBB4	erb-b2 receptor tyrosine kinase 4	3432	2066	ENSG00000178568
FOXP1	forkhead box P1	3823	27086	ENSG00000114861
GAD1	glutamate decarboxylase 1 (brain. 67kDa)	4092	2571	ENSG00000128683
MAPK14	mitogen-activated protein kinase 14	6876	1432	ENSG00000112062
MECP2	methyl CpG binding protein 2	6990	4204	ENSG00000169057
MEF2A	myocyte enhancer factor 2A	6993	4205	ENSG00000068305
MET	MET proto-oncogene. receptor tyrosine kinase	7029	4233	ENSG00000105976
NRG1	neuregulin 1	7997	3084	ENSG00000157168
NCAM1	neural cell adhesion molecule 1	7656	4684	ENSG00000149294
POU3F2	POU class 3 homeobox 2	9215	5454	ENSG00000184486
RELN	reelin	9957	5649	ENSG00000189056
ROBO1	roundabout. axon guidance receptor. homolog 1 (Drosophila)	10249	6091	ENSG00000169855
ROBO2	roundabout. axon guidance receptor. homolog 2 (Drosophila)	10250	6092	ENSG00000185008
SIRT1	sirtuin 1	14929	23411	ENSG0000009671
SOX10	SRY (sex determining region Y)-box 10	11190	6663	ENSG0000010014

¹Gene symbol according to the Hugo Gene Nomenclature Committee (HGNC; https://www.genenames.org).

²Identifier (ID) from HGNC for genes with an approved gene symbol.

³Identifier (ID) from ENTREZ, an online cross-database search system from the National Center for Biotechnology Information (NCBI), USA.

⁴Identifier (ID) from ENSEMBL, the European equivalent to ENTREZ from the European Bioinfomatics Institute and the Wellcome Trust Sanger Institute.

Supplementary Table 4. Gene expression analysis – 14 color genes used as negative control

Gene ¹	HGNC ID ²	ENTREZ ID ³	ENSEMBL ID ⁴
ASIP	745	434	ENSG00000101440
BNC2	30988	54796	ENSG00000173068
EIF2S2	3266	8894	ENSG00000125977
GSS	4624	2937	ENSG00000100983
HERC2	4868	8924	ENSG00000128731
IRF4	6119	3662	ENSG00000137265
MC1R	6929	4157	ENSG00000258839
OCA2	8101	4948	ENSG00000104044
RALY	15921	22913	ENSG00000125970
SLC24A4	10978	123041	ENSG00000140090
SLC24A5	20611	283652	ENSG00000188467
SLC45A2	16472	51151	ENSG00000164175
TYR	12442	7299	ENSG00000077498
VASH2	25723	79805	ENSG00000143494

¹Gene symbol according to the Hugo Gene Nomenclature Committee (HGNC; https://www.genenames.org).

²Identifier (ID) from HGNC for genes with an approved gene symbol.

³Identifier (ID) from ENTREZ, an online cross-database search system from the National Center for Biotechnology Information (NCBI). USA.

⁴Identifier (ID) from ENSEMBL, the European equivalent to ENTREZ from the European Bioinformatics Institute and the Wellcome Trust Sanger Institute.

Supplementary Table 5. Main expression analysis of the candidate genes in left area 44 (versus left premotor region)

	Expression levels (mean z-	score and standard deviation)	
_	Left area 44	Left premotor region	
Gene	Mean (SD)	Mean (SD)	p-value
MET	-0.097 (0.282)	-0.592 (0.348)	0.001*
CNTNAP2	0.452 (0.265)	0.306 (0.217)	0.038
NRG1	-0.007 (0.128)	0.147 (0.238)	0.054
POU3F2	-0.189 (0.261)	-0.006 (0.284)	0.065
SOX10	0.075 (0.321)	0.357 (0.450)	0.107
ROBO2	0.307 (0.387)	0.110 (0.319)	0.122
DISC1	-0.489 (0.295)	-0.381 (0.301)	0.188
SIRT1	-0.480 (0.453)	-0.621 (0.358)	0.193
RELN	-0.147 (0.492)	-0.317 (0.306)	0.233
NCAM1	-0.330 (0.483)	-0.156 (0.447)	0.293
ROBO1	-0.416 (0.313)	-0.520 (0.352)	0.298
MECP2	-0.446 (0.415)	-0.306 (0.597)	0.444
MEF2A	0.305 (0.351)	0.148 (0.433)	0.528
ERBB4	0.168 (0.400)	0.171 (0.410)	0.608
FOXP1	0.019 (0.291)	-0.031 (0.293)	0.711
AKT1	0.263 (0.384)	0.187 (0.448)	0.836
GAD1	0.299 (0.190)	0.304 (0.163)	0.866
ELAVL2	0.196 (0.328)	0.200 (0.271)	0.867
CDC42	-0.148 (0.355)	-0.146 (0.342)	0.971
MAPK14	0.231 (0.464)	0.152 (0.413)	0.973

Analyses were performed using a permuted n-way ANOVA.

^{*}Stable against correction for multiple comparisons (family-wise error).

Supplementary Table 6. Main expression analysis of the candidate genes in left area 45 (versus left premotor region)

	Expression levels (mean z-		
	Left area 45	Left premotor region	
Gene	Mean (SD)	Mean (SD)	<i>p</i> -value
MET	0.102 (0.243)	-0.592 (0.348)	0.000*
SIRT1	-0.230 (0.350)	-0.621 (0.358)	0.003*
CNTNAP2	0.501 (0.225)	0.306 (0.217)	0.005
FOXP1	0.213 (0.267)	-0.031 (0.293)	0.012
ELAVL2	-0.015 (0.274)	0.200 (0.271)	0.034
ROBO2	-0.189 (0.426)	0.110 (0.319)	0.055
NRG1	-0.003 (0.181)	0.147 (0.238)	0.074
ERBB4	0.032 (0.489)	0.171 (0.410)	0.187
NCAM1	-0.305 (0.520)	-0.156 (0.447)	0.411
RELN	-0.205 (0.387)	-0.317 (0.306)	0.450
GAD1	0.326 (0.130)	0.304 (0.163)	0.487
AKT1	0.362 (0.268)	0.187 (0.448)	0.509
MEF2A	0.296 (0.292)	0.148 (0.433)	0.539
MECP2	-0.418 (0.563)	-0.306 (0.597)	0.595
DISC1	-0.320 (0.355)	-0.381 (0.301)	0.608
SOX10	0.264 (0.411)	0.357 (0.450)	0.895
POU3F2	-0.042 (0.295)	-0.006 (0.284)	0.911
MAPK14	0.210 (0.518)	0.152 (0.413)	0.931
ROBO1	-0.540 (0.415)	-0.520 (0.352)	0.952
CDC42	-0.186 (0.327)	-0.146 (0.342)	0.995

Analyses were performed using a permuted n-way ANOVA.

^{*}Stable against correction for multiple comparisons (family-wise error).

Supplementary Table 7. Main expression analysis of the candidate genes in right area 44 (versus right premotor region)

Expression levels (mean z-score and standard deviation)			
	Right area 44	Right premotor region	
Gene	Mean (SD)	Mean (SD)	<i>p</i> -value
MET	0.091 (0.213)	-0.572 (0.459)	0.014
MECP2	-0.615 (0.302)	-0.267 (0.347)	0.115
GAD1	0.339 (0.063)	0.457 (0.159)	0.135
ELAVL2	0.030 (0.288)	0.269 (0.243)	0.149
POU3F2	-0.294 (0.093)	-0.083 (0.253)	0.157
ROBO2	0.036 (0.524)	0.386 (0.351)	0.179
RELN	-0.486 (0.205)	-0.152 (0.496)	0.259
MAPK14	0.151 (0.486)	0.325 (0.338)	0.420
NRG1	-0.070 (0.191)	0.053 (0.237)	0.444
NCAM1	-0.501 (0.281)	-0.271 (0.529)	0.461
DISC1	-0.606 (0.209)	-0.519 (0.182)	0.480
ERBB4	0.083 (0.433)	0.313 (0.540)	0.486
SIRT1	-0.294 (0.179)	-0.429 (0.326)	0.505
MEF2A	0.280 (0.356)	0.229 (0.404)	0.507
CNTNAP2	0.492 (0.082)	0.433 (0.184)	0.575
AKT1	0.212 (0.511)	0.144 (0.574)	0.712
CDC42	-0.101 (0.283)	-0.146 (0.341)	0.785
ROBO1	-0.692 (0.254)	-0.654 (0.321)	0.861
FOXP1	-0.017 (0.320)	0.039 (0.361)	0.872
SOX10	-0.095 (0.748)	-0.076 (0.667)	0.990

Analyses were performed using a permuted *n*-way ANOVA.

No p-value was stable against correction for multiple comparisons (family-wise error).

Supplementary Table 8. Main expression analysis of the candidate genes in right area 45 (versus right premotor region)

-	Expression levels (mean z-score and standard deviation)		
•	Right area 45	Right premotor region	
Gene	Mean (SD)	Mean (SD)	p-value
MET	0.269 (0.204)	-0.572 (0.459)	0.001*
ROBO2	-0.029 (0.367)	0.386 (0.351)	0.059
NRG1	-0.170 (0.111)	0.053 (0.237)	0.063
MECP2	-0.683 (0.394)	-0.267 (0.347)	0.064
CNTNAP2	0.625 (0.182)	0.433 (0.184)	0.066
ELAVL2	0.037 (0.263)	0.269 (0.243)	0.125
MAPK14	0.056 (0.360)	0.325 (0.338)	0.182
SIRT1	-0.212 (0.185)	-0.429 (0.326)	0.183
DISC1	-0.640 (0.162)	-0.519 (0.182)	0.242
NCAM1	-0.601 (0.298)	-0.271 (0.529)	0.270
FOXP1	-0.197 (0.299)	0.039 (0.361)	0.293
GAD1	0.360 (0.104)	0.457 (0.159)	0.295
POU3F2	-0.240 (0.206)	-0.083 (0.253)	0.316
AKT1	0.209 (0.657)	0.144 (0.574)	0.490
RELN	-0.015 (0.339)	-0.152 (0.496)	0.561
ERBB4	0.098 (0.455)	0.313 (0.540)	0.606
ROBO1	-0.736 (0.217)	-0.654 (0.321)	0.607
CDC42	-0.250 (0.196)	-0.146 (0.341)	0.615
MEF2A	0.122 (0.291)	0.229 (0.404)	0.940
SOX10	-0.104 (0.586)	-0.076 (0.667)	0.976

Analyses were performed using a permuted n-way ANOVA.

^{*}Stable against correction for multiple comparisons (family-wise error).

Supplementary Table 9. Follow-up gene expression analysis of color genes in left area 44 (versus left premotor region)

•	O ,				
	Expression levels (mean z-score and standard deviation)				
	Left area 44	Left premotor region			
Gene	Mean (SD)	Mean (SD)	p-value		
SLC24A4	0.350 (0.259)	-0.019 (0.344)	0.002*		
OCA2	0.662 (0.288)	0.396 (0.412)	0.029		
IRF4	-0.481 (0.343)	-0.069 (0.515)	0.030		
VASH2	-0.252 (0.673)	0.121 (0.482)	0.114		
MC1R	-0.176 (0.304)	-0.312 (0.273)	0.149		
GSS	0.493 (0.268)	0.309 (0.352)	0.190		
BNC2	-0.435 (0.300)	-0.290 (0.325)	0.228		
SLC24A5	-0.099 (0.483)	-0.324 (0.464)	0.314		
HERC2	0.069 (0.488)	0.200 (0.551)	0.578		
EIF2S2	0.079 (0.197)	-0.010 (0.332)	0.664		
TYR	0.003 (0.473)	0.151 (1.110)	0.799		
SLC45A2	-0.095 (0.711)	-0.173 (0.650)	0.873		
RALY	0.598 (0.224)	0.593 (0.429)	0.899		
ASIP	-0.266 (0.516)	-0.312 (0.376)	0.955		

Analyses were performed using a permuted *n*-way ANOVA.

Supplementary Table 10. Follow-up gene expression analysis of color genes in left area 45 (versus left premotor region)

	t promotor region,		
	Expression levels (mean z-	score and standard deviation)	
	Left area 45	Left premotor region	
Gene	Mean (SD)	Mean (SD)	p-value
SLC24A4	0.408 (0.389)	-0.019 (0.344)	0.009
VASH2	-0.418 (0.399)	0.121 (0.482)	0.010
OCA2	0.642 (0.415)	0.396 (0.412)	0.043
HERC2	0.578 (0.676)	0.200 (0.551)	0.060
MC1R	-0.074 (0.431)	-0.312 (0.273)	0.090
GSS	0.599 (0.436)	0.309 (0.352)	0.108
IRF4	-0.431 (0.719)	-0.069 (0.515)	0.161
BNC2	-0.419 (0.246)	-0.290 (0.325)	0.305
SLC24A5	-0.171 (0.484)	-0.324 (0.464)	0.391
EIF2S2	0.091 (0.466)	-0.010 (0.332)	0.444
ASIP	-0.374 (0.584)	-0.312 (0.376)	0.521
RALY	0.679 (0.559)	0.593 (0.429)	0.666
SLC45A2	-0.215 (0.564)	-0.173 (0.650)	0.834
TYR	0.110 (0.536)	0.151 (1.110)	0.989

Analyses were performed using a permuted *n*-way ANOVA.

No p-value was stable against correction for multiple comparisons (family-wise error).

^{*}Stable against correction for multiple comparisons (family-wise error).

Supplementary Table 11. Follow-up gene expression analysis of color genes in right area 44 (versus right premotor region)

	Expression levels (mean z-score and standard deviation)		
	Right area 44	Right premotor region	
Gene	Mean (SD)	Mean (SD)	p-value
VASH2	-0.561 (0.150)	0.178 (0.455)	0.007
BNC2	0.150 (0.507)	-0.342 (0.480)	0.119
ASIP	0.269 (0.368)	-0.292 (0.626)	0.145
SLC24A4	0.509 (0.371)	0.137 (0.464)	0.154
OCA2	0.945 (0.276)	0.475 (0.560)	0.164
GSS	0.506 (0.541)	0.186 (0.443)	0.218
RALY	0.659 (0.332)	0.300 (0.713)	0.334
IRF4	-0.511 (0.426)	-0.170 (0.839)	0.531
MC1R	-0.255 (0.644)	-0.379 (0.439)	0.585
EIF2S2	0.153 (0.429)	0.077 (0.431)	0.710
HERC2	0.107 (0.629)	0.025 (0.795)	0.786
TYR	-0.470 (0.327)	-0.467 (0.370)	0.979
SLC24A5	-0.033 (0.310)	-0.040 (0.355)	0.981
SLC45A2	-0.012 (0.605)	-0.015 (0.845)	0.988

Analyses were performed using a permuted *n*-way ANOVA.

No p-value was stable against correction for multiple comparisons (family-wise error).

Supplementary Table 12. Follow-up gene expression analysis of color genes in right area 45 (versus right premotor region)

10 (101040119	Expression levels (mean z-score and standard deviation)		
·	Right area 45	Right premotor region	
Gene	Mean (SD)	Mean (SD)	p-value
VASH2	-0.427 (0.189)	0.178 (0.455)	0.006
SLC24A4	0.566 (0.455)	0.137 (0.464)	0.045
RALY	0.675 (0.426)	0.300 (0.713)	0.209
GSS	0.361 (0.482)	0.186 (0.443)	0.325
ASIP	0.015 (0.432)	-0.292 (0.626)	0.345
OCA2	0.720 (0.415)	0.475 (0.560)	0.408
TYR	-0.333 (0.371)	-0.467 (0.370)	0.419
HERC2	0.111 (0.685)	0.025 (0.795)	0.636
SLC45A2	0.103 (0.870)	-0.015 (0.845)	0.711
SLC24A5	0.035 (0.299)	-0.040 (0.355)	0.721
IRF4	-0.308 (0.436)	-0.170 (0.839)	0.722
MC1R	-0.402 (0.495)	-0.379 (0.439)	0.769
EIF2S2	0.081 (0.405)	0.077 (0.431)	0.821
BNC2	-0.340 (0.286)	-0.342 (0.480)	0.881

Analyses were performed using a permuted *n*-way ANOVA.

No p-value was stable against correction for multiple comparisons (family-wise error).

Supplementary Table 13. Gene expression analysis of FOXP2 in left area 44 (versus left

premotor region)

	Expression levels (mean z-score and standard deviation)		
	Left area 44	Left premotor region	
Gene	Mean (SD)	Mean (SD)	p-value
FOXP2	0.317 (0.237)	0.067 (0.336)	0.015

Analyses were performed using a permuted *n*-way ANOVA.

Supplementary Table 14. Gene expression analysis of FOXP2 in left area 45 (versus left

premotor region)

	Expression levels (mean z-score and standard deviation)		
	Left area 45	Left premotor region	
Gene	Mean (SD)	Mean (SD)	p-value
FOXP2	0.249 (0.448)	0.067 (0.336)	0.201

Analyses were performed using a permuted *n*-way ANOVA.

Supplementary Table 15. Gene expression analysis of FOXP2 in right area 44 (versus right premotor region)

right promoter region,				
	Expression levels (mean z-score and standard deviation)			
	Right area 44	Right premotor region		
Gene	Mean (SD)	Mean (SD)	p-value	
FOXP2	0.442 (0.209)	0.073 (0.441)	0.106	

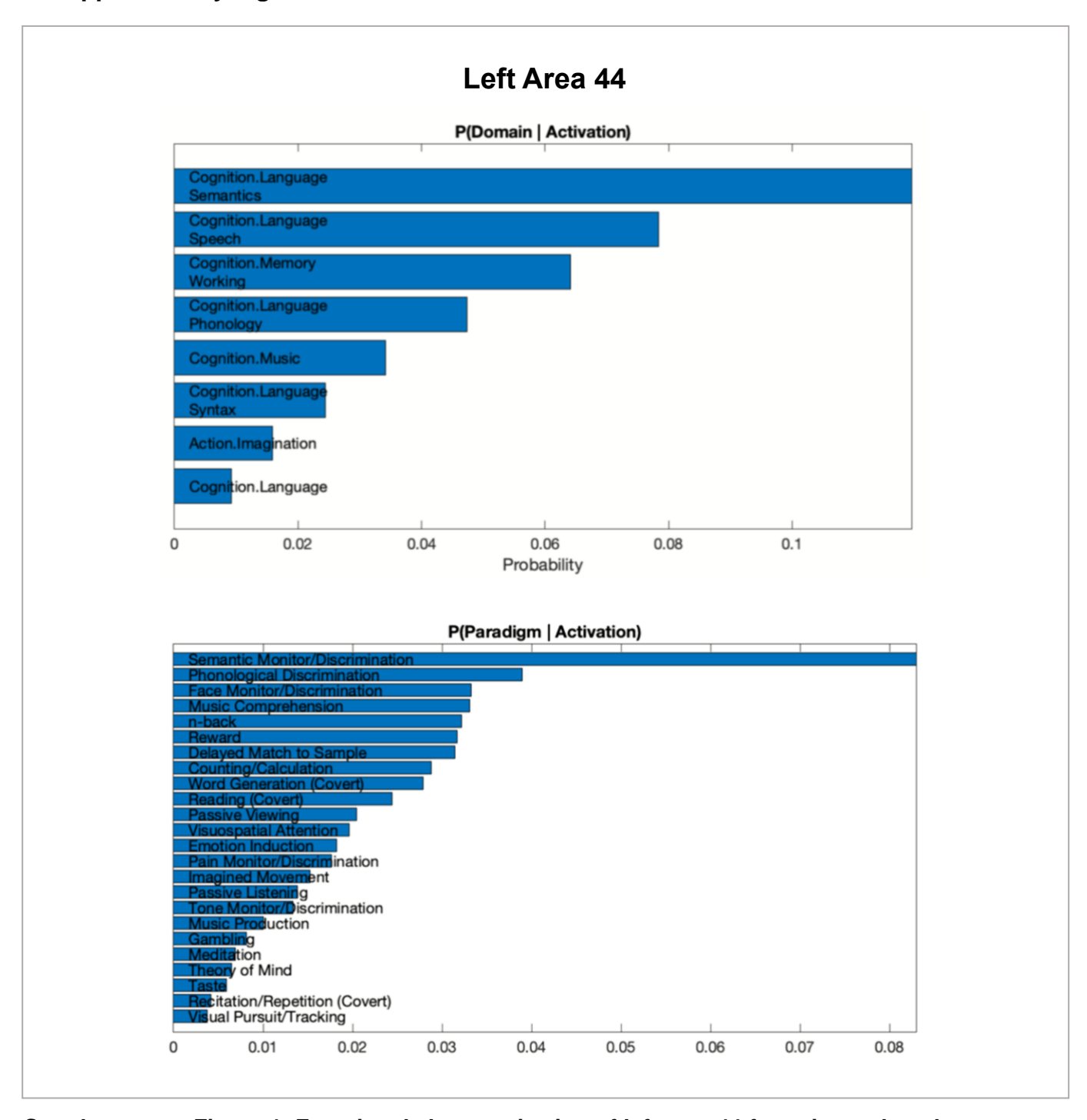
Analyses were performed using a permuted *n*-way ANOVA.

Supplementary Table 16. Gene expression analysis of FOXP2 in right area 45 (versus right premotor region)

	Expression levels (mean z-score and standard deviation)		
	Right area 45	Right premotor region	
Gene	Mean (SD)	Mean (SD)	p-value
FOXP2	0.282 (0.339)	0.073 (0.441)	0.225

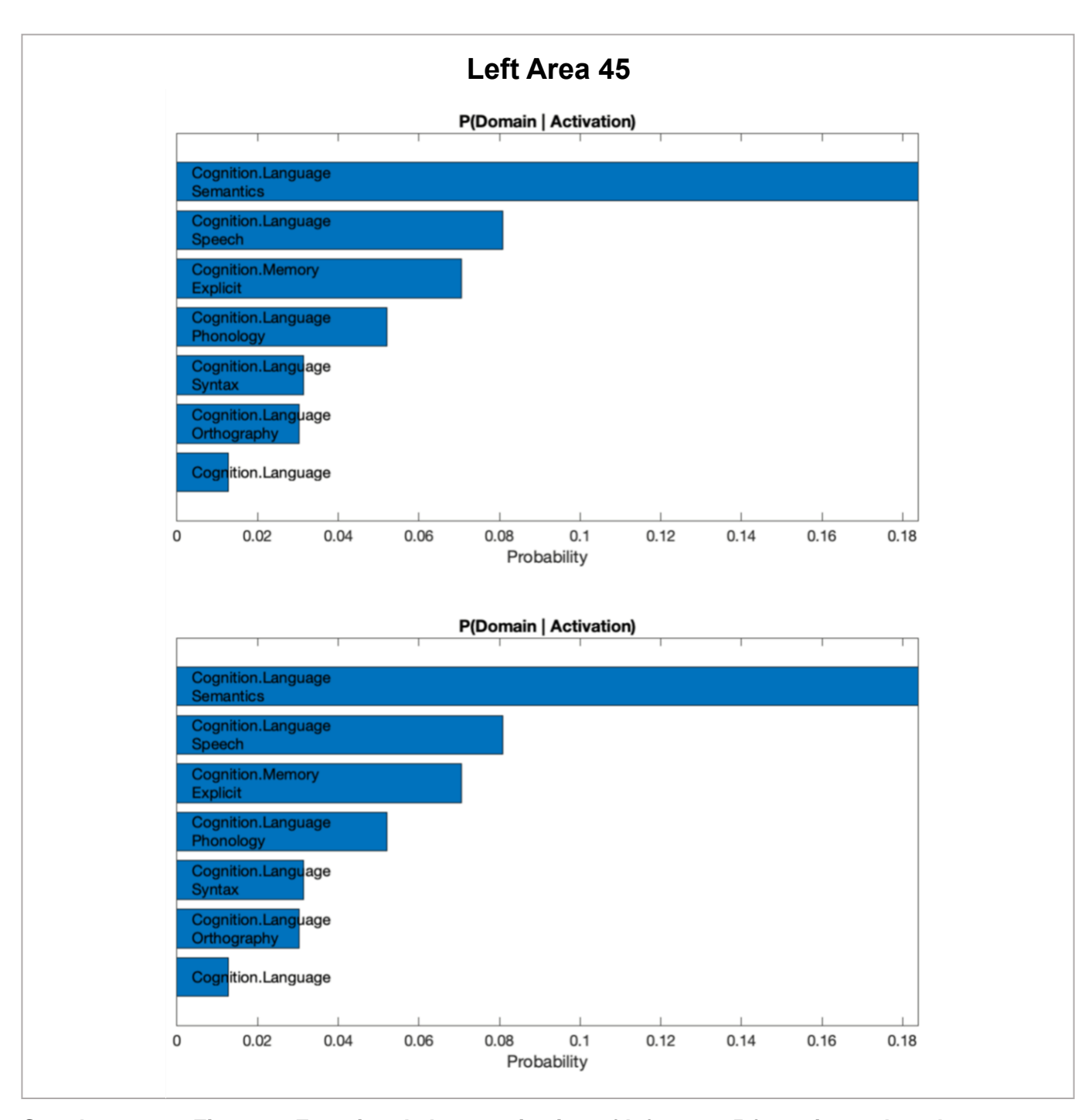
Analyses were performed using a permuted *n*-way ANOVA.

Supplementary Figures



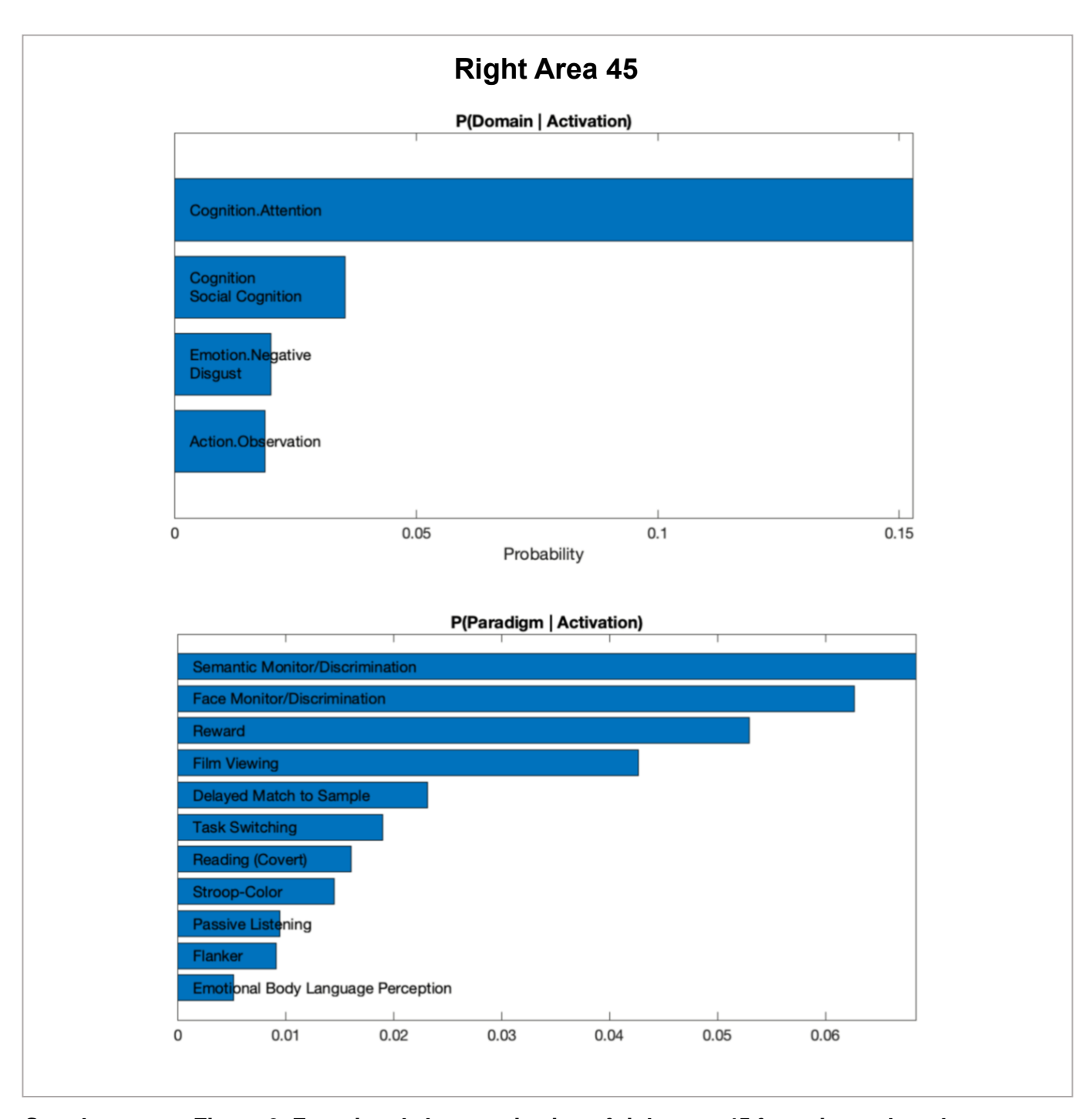
Supplementary Figure 1. Functional characterization of left area 44 featuring reduced gray matter associated with the negative symptom dimension in schizophrenia.

Significant associations with psychological terms (behavioral domains and paradigm classes) from BrainMap metadata. We used a reverse inference approach (P(Domain/Paradigm | Activation)) that determined the above-chance probability of association with a behavioral function given observed brain activity in the respective region. The base rate denotes the general probability of finding BrainMap activation in the region. The x-axis indicates relative probability values.



Supplementary Figure 2. Functional characterization of left area 45 featuring reduced gray matter associated with the negative symptom dimension in schizophrenia.

Significant associations with psychological terms (behavioral domains and paradigm classes) from BrainMap metadata. We used a reverse inference approach (P(Domain/Paradigm | Activation)) that determined the above-chance probability of association with a behavioral function given observed brain activity in the respective region. The base rate denotes the general probability of finding BrainMap activation in the region. The x-axis indicates relative probability values.



Supplementary Figure 3. Functional characterization of right area 45 featuring reduced gray matter associated with the cognitive symptom dimension in schizophrenia.

Significant associations with psychological terms (behavioral domains and paradigm classes) from BrainMap metadata. We used a reverse inference approach (P(Domain/Paradigm | Activation)) that determined the above-chance probability of association with a behavioral function given observed brain activity in the respective region. The base rate denotes the general probability of finding BrainMap activation in the region. The x-axis indicates relative probability values.

Supplementary References

- 1. Aine, C.J., et al. Multimodal neuroimaging in schizophrenia: description and dissemination. Neuroinformatics 15, 343-364 (2017).
- 2. Poeppl, T.B., *et al.* Amygdalohippocampal neuroplastic changes following neuroleptic treatment with quetiapine in first-episode schizophrenia. *Int J Neuropsychopharmacol* **17**, 833-843 (2014).
- 3. Schilbach, L., *et al.* Differential patterns of dysconnectivity in mirror neuron and mentalizing networks in schizophrenia. *Schizophr Bull* **42**, 1135-1148 (2016).
- 4. Chahine, G., Richter, A., Wolter, S., Goya-Maldonado, R. & Gruber, O. Disruptions in the left frontoparietal network underlie resting state endophenotypic markers in schizophrenia. *Hum Brain Mapp* **38**, 1741-1750 (2017).
- 5. Vercammen, A., Knegtering, H., den Boer, J.A., Liemburg, E.J. & Aleman, A. Auditory hallucinations in schizophrenia are associated with reduced functional connectivity of the temporo-parietal area. *Biol Psychiatry* **67**, 912-918 (2010).
- 6. Clos, M., Diederen, K.M., Meijering, A.L., Sommer, I.E. & Eickhoff, S.B. Aberrant connectivity of areas for decoding degraded speech in patients with auditory verbal hallucinations. *Brain Struct Funct* **219**, 581-594 (2014).
- 7. Collinson, S.L., *et al.* Corpus callosum morphology in first-episode and chronic schizophrenia: combined magnetic resonance and diffusion tensor imaging study of Chinese Singaporean patients. *Br J Psychiatry* **204**, 55-60 (2014).
- 8. Sorg, C., et al. Increased intrinsic brain activity in the striatum reflects symptom dimensions in schizophrenia. *Schizophr Bull* **39**, 387-395 (2013).
- 9. Lefebvre, S., *et al.* Network dynamics during the different stages of hallucinations in schizophrenia. *Hum Brain Mapp* **37**, 2571-2586 (2016).
- Koutsouleris, N., et al. Predicting Response to Repetitive Transcranial Magnetic Stimulation in Patients With Schizophrenia Using Structural Magnetic Resonance Imaging: A Multisite Machine Learning Analysis. Schizophr Bull 44, 1021-1034 (2018).

- 11. Wobrock, T., *et al.* Left prefrontal high-frequency repetitive transcranial magnetic stimulation for the treatment of schizophrenia with predominant negative symptoms: a sham-controlled, randomized multicenter trial. *Biol Psychiatry* **77**, 979-988 (2015).
- 12. Soler-Vidal, J., *et al.* Brain correlates of speech perception in schizophrenia patients with and without auditory hallucinations. *PLoS One* **17**, e0276975 (2022).
- 13. Murphy, E. & Benítez-Burraco, A. Bridging the gap between genes and language deficits in schizophrenia: An oscillopathic approach. *Front Hum Neurosci* **10**, 422 (2016).